Biomedicine & Pharmacotherapy 151 (2022) 113137

Contents lists available at ScienceDirect

Biomedicine & Pharmacotherapy

journal homepage: www.elsevier.com/locate/biopha

Endogenous and exogenous hydrogen sulfide modulates urothelial bladder carcinoma development in human cell lines

Elisabetta Panza [a,*], Ivana Bello [a], Martina Smimmo [a], Vincenzo Brancaleone [b], Emma Mitidieri [a], Mariarosaria Bucci [a], Giuseppe Cirino [a], Raffaella Sorrentino [c,1], Roberta d'Emmanuele di Villa Bianca [a,1]

[a] Department of Pharmacy, School of Medicine and Surgery, University of Naples Federico II, Naples, Italy
[b] Department of Science, University of Basilicata, Potenza, Italy
[c] Department of Molecular Medicine and Medical Biotechnology, School of Medicine, University of Naples, Federico II, Italy

ARTICLE INFO

Keywords:
Hydrogen sulfide
Urothelial carcinoma
Apoptosis
Autophagy
Epithelial-mesenchymal transition

ABSTRACT

The role of H_2S in urothelial carcinoma (UC) is still unclear. Here we have evaluated the expression of H_2S producing enzymes as well as the effect of endogenous and exogenous H_2S on human bladder UC cells. In human UC cells the expression of cystathionine β-synthase (CBS), cystathionine γ-lyase (CSE), and 3-mercaptopyruvate sulfurtransferase (3-MST); is significantly lower as compared to healthy cells. A modulatory role for the H_2S pathway is supported by the finding that, the overexpression of CSE or CBS, but not 3-MST, inhibits cell proliferation and promotes apoptosis. A similar effect is obtained by using exogenous H_2S. Diallyl trisulfide (DATS), which is a fully characterized H_2S donor, inhibits the proliferation of UC cells in a time and concentration-dependent manner as well as promotes apoptosis. Moreover, DATS also induces autophagy, as determined by transcriptomic and western blot analysis. Finally, DATS inhibits mRNA expression levels of canonical markers of epithelial-mesenchymal transition by limiting migration and clonogenic ability of human UC cells in vitro. In conclusion, in urothelial carcinoma, there is an impairment of H_2S pathway that involves CSE and CBS- derived hydrogen sulfide. Thus, targeting H_2S signaling pathway in urothelial carcinoma could represent a novel therapeutic strategy.

1. Introduction

Urothelial carcinoma (UC), also known as transitional cell carcinoma, is the most common type of bladder cancer with a frequency of about 90% among upper urinary tract tumors [1]. It is frequently associated with harmful chemical exposure including chemicals in tobacco smoke. About 70% of patients with UC present a non-muscle invasive disease that, although is often recurring, is generally not life-threatening. While in the remaining 30% of patients, the disease is muscle-invasive causing high mortality due to the occurrence of metastasis [2]. Currently, the standard cure for UC relies on surgical (radical cystectomy) and/or pharmacological treatments with (neo-) adjuvant chemo drugs or recently approved immune checkpoint inhibitors. Chemotherapy mostly relies on the combination of cisplatin with other cytotoxic drugs. However, it is estimated that only about 30–50% of patients generally respond well to the drugs, while the majority of them become refractory during the treatment with a five-year survival rate below 30–40% [3]. Yet, also with the advent of novel immunotherapeutic treatments, the outcome for patients is not significantly changed [4,5].

Hydrogen sulfide (H_2S), together with nitric oxide and carbon monoxide, is a key gas signaling molecule playing an important role in cellular processes underlying cancer development and progression including angiogenesis, oxidative stress, cell cycle, autophagy, apoptosis, epithelial-mesenchymal transition, protein sulfhydration and chemotherapy resistance [6–8]. H_2S is known to be endogenously produced by several enzymes, including cystathionine β-synthase (CBS), cystathionine γ-lyase (CSE), the tandem enzymes cysteine

Abbreviations: H_2S, Hydrogen sulfide; UC, urothelial carcinoma; CBS, cystathionine β-synthase; CSE, cystathionine γ-lyase; 3-MST, 3-mercaptopyruvate sulfurtransferase; DATS, diallyl trisulfide; EMT, Epithelial-to-mesenchymal transition.

* Correspondence to: Department of Pharmacy, School of Medicine and Surgery, University of Naples Federico II, Via Domenico Montesano 49, 80131 Naples, Italy.
E-mail address: e.panza@unina.it (E. Panza).

[1] These authors contributed equally to this work.

https://doi.org/10.1016/j.biopha.2022.113137

Available online 24 May 2022

aminotransferase (CAT), and 3-mercaptopyruvate sulfurtransferase (3-MST) [9]. Accumulating evidence demonstrated that CSE, CBS, and 3-MST regulate numerous physiological functions in the brain as well as peripheral organs and tissues. As a consequence, the dysregulation of these enzymes is associated with several disorders including several forms of cancer. In this regard, CSE, CBS, and 3-MST to a different extent, were found dysregulated in colon, prostate, breast, renal, urothelial, ovarian, melanoma, oral squamous, and thyroid cancer [10–14]. In general, the overactivity of these enzymes has been associated with a poor prognosis and higher tumor invasiveness [15–17]. Although the role of endogenous H_2S in tumors is still controversial, the relatively high concentration of exogenous H_2S can mainly suppress the growth of cancer cells [6]. The response of cancer cells to H_2S donors varies substantially depending on the donor type, concentration, and cancer type. In any case, the anticancer role of H_2S is known to be mostly exerted through the regulation of (i) immune responses [18,19], (ii) activity of numerous genes as well as transcription factors including NF-κB [20], STAT-3 [21], and Nrf-2 [22,23]; (iii) cell cycle [24], (iv) cell migration and invasion [25], (v) autophagy and apoptosis [26,27]. However, the exact molecular mechanism underlying the H_2S anticancer effect in urothelial carcinoma cells is still unclear. In this line, the present study aims at evaluating the expression and role of CBS, CSE, and 3-MST in human UC cells. In addition, the potential anticancer effect of exogenous H_2S was examined by investigating cell cycle regulation, autophagy, apoptosis, and epithelial-mesenchymal transition.

2. Materials and methods

2.1. Cell culture and reagents

SVHUC1 (cat. CRL-9520), T24 (cat. HTB-4) and UMUC3 (cat. CRL-1749) cells were purchased from the American Type Culture Collection (ATCC, Manassas, VA, USA). Cell lines were used between passages 3 and 10. SVHUC1 cells were grown in HAM'S F12 medium (cat. 11765054, Thermo Fisher Scientific, MA, USA) containing 10% fetal bovine serum, 2 mmol/l L-glutamine, penicillin (100 U/ml), streptomycin (100 mg/ml) (all from Merk, Milan, Italy). T24 cells were grown in MC COY'S (cat. 16600082, Thermo Fisher Scientific, MA, USA) and UMUC3 cells in EMEM medium (cat. 10-009-CV, Corning®, AZ, USA), both media were supplemented with 10% fetal bovine serum, 2 mmol/l L-glutamine, penicillin (100 U/ml), streptomycin (100 μg/ml) and 1 mmol/L sodium pyruvate (all from Merk, Milan, Italy). Cells were maintained in a humified incubator at 37 °C with 5% CO_2. DATS (cat. SMB00577) was purchased from Merk (Italy); GYY4137 (cat. 13345) from Cayman Chemical (MI, USA).

2.2. Western blot analysis

Total proteins were extracted from cells using a lysis RIPA buffer (50 mM Tris-HCl (pH 7.4), 1 mM EDTA, 150 mM NaCl, 1% Triton X-100, 0,25% (v/v) sodium deoxycholate, 0,1% SDS) supplemented with Protease Inhibitor Cocktail (cat. P8340-1 ml, Merk, Milan, Italy). Protein concentration was then measured by the Bradford method (Cat. 5000006, Bio-Rad, Italy). An equal amount of proteins (40 μg) from each cell extract was loaded and separated on sodium dodecyl sulfate polyacrylamide (SDS-PAGE) gel and subsequently transferred from the gel onto a nitrocellulose membrane using Trans-Blot Turbo Transfer Starter System (Bio-Rad, Italy). After transfer, the membranes were blocked in 5% low-fat milk in PBS with 0,1% Tween 20 (PBST) for 1 h at room temperature and then incubated overnight at 4 °C with the following primary antibodies (i) CBS (cat. 14787-1-AP, Proteintech Group, Chicago, IL; diluted 1: 1000); (ii) CSE (cat. 60234-1-Ig, Proteintech Group, Chicago, IL; diluted 1: 1000); (iii) 3-MST (cat. sc-135993, Santa Cruz Biotechnology, Santa Cruz, CA; diluted 1:1000); (iv) Caspase 3 (cat. 9662, Cell Signaling, MA, USA; diluted 1: 1000); (v) PARP (cat. 9542, Cell Signaling, MA, USA; diluted 1: 1000); (vi) XIAP (cat. AF8221, R&D Systems, MN, USA; concentrated 1 μg/ml); (vii) Bcl-2 (cat. 2876, Cell Signaling, MA, USA; diluted 1: 1000); (viii) Cyclin D1 (cat. 2922, Cell Signaling, MA, USA; diluted 1:1000); (ix) CDK4 (cat. 12790, Cell Signaling, MA, USA; diluted 1:1000); (x) LC3 (cat. 2775, Cell Signaling, MA, USA; diluted 1:1000); (xi) p62 (cat. 5115, Cell Signaling, MA, USA; diluted 1:1000); (xii) E-Cadherin (cat. 3195, Cell Signaling, MA, USA; diluted 1:1000); (xiii) Caveolin-1 (cat. 3238, Cell Signaling, MA, USA; diluted 1:1000); (xiv) Vimentin (cat. sc-373717, Santa Cruz Biotechnology, Santa Cruz, CA; diluted 1:1000). Following the incubation, primary antibodies were removed, and membranes washed three times with PBST. Anti-mouse (cat. 115-035-003) and/or anti-rabbit (cat. 111-035-144) IgG secondary antibodies (Jackson ImmunoResearch, Cambridge, UK, dilution 1: 3000) for 1.30 h at room temperature. An antibody anti GAPDH protein (cat. 1E6D9, Proteintech Group, Chicago, IL; diluted 1: 5000) was used as the control normalizing protein [28]. Following incubation, secondary antibodies were removed, and membranes washed three times with PBST. Protein bands were detected by using the enhanced chemiluminescence method (Clarity TM Western ECL Substrate, cat. 1705061, Bio-Rad Laboratories, CA, USA) and Chemidoc XRS (Biorad, Milan, Italy). Quantification of results was made using ImageJ Software (version 1.52a, U.S. National Institutes of Health).

Table 1
List of primers used in qPCR analysis.

Gene	FORWARD Sequence (5′->3′)	REVERSE Sequence (5′->3′)
Human		
CBS	GGCCAAGTGTGAGTTCTTCAA	GGCTCGATAATCGTGTCCCC
CSE	AGGTTTAGCAGCCACTGTAAC	GGGGTTTCGATCCAAACAAGC
3-MST	CATTTCGCGGAGTACGCAG	GCTGGCGTCGTAGATCACG
S16	TACCACGGAGGCCACCTAA	CTGCTCCACAAATCGGCCAT
ATG13	TTGCTATAACTAGGGTGACACCA	CCCAACACGAACTGTCTGGA
BECN1	ACCTCAGCCGAAGACTGAAG	AACAGCGTTTGTAGTTCTGACA
BNIP3	ATGTCGTCCCACCTAGTCGAG	TGAGGATGGTACGTGTTCCAG
LAMP1	TCTCAGTGAACTACGACACCA	AGTGTATGTCCTCTTCCAAAAGC
ULK1	AGCACGATTTGGAGGTCGC	GCCACGATGTTTTCATGTTTCA
mTOR	TCCGAGAGATGAGTCAAGAGG	CACCTTCCACTCCTATGAGGC
SLUG	CGAACTGGACACACATACAGTG	CTGAGGATCTCTGGTTGTGGT
ZEB1	TTACACCTTTGCATACAGAACCC	TTTACGATTACACCCAGACTGC

2.3. RNA purification and quantitative real-time PCR

Total RNA was isolated from cells using the QIAzol Lysis Reagent according to the manufacturer's instructions (Cat. 79306, Qiagen, Hilden, Germany). The purity and quantity of each purified RNA were evaluated considering the ratio between readings at 260/280 nm using an Eppendorf BioPhotometer and Nanodrop apparatus (Thermo Fisher Scientific, MA, USA). Purified mRNA was reverse-transcribed using iScript Reverse Transcription Supermix for RT-qPCR (cat. 1708841, Bio-Rad, Italy). qPCR was carried out in a CFX96 real-time PCR detection system (Bio-Rad) with the use of specific primers (Table 1) and SYBR Green master mix kit (cat. 1725271, Bio-Rad). Real-Time PCR cycling protocol was: Polymerase Activation and DNA Denaturation 95 °C for 30 s, Amplification 40 cycles, Denaturation 95 °C for 15 s, Annealing and Extension 60 °C for 30 s, Plate read at 60 °C, Melt-Curve Analysis 65–95 °C 0.5 °C increment, 5 s/step. The housekeeping gene (ribosomal protein S16) was used as an internal control to normalize the CT values, using the $2^{-\Delta\Delta Ct}$ formula.

2.4. Transfection

The day before, UMUC3 cells were seeded onto 96-well plates (2×10^3 cell/well) and 6-well plates (3×10^5 cell/well). After 24 h, cells were transfected (at a confluence of about 60–70%) with the following plasmids: (i) human CSE/pIRES-EGFP, (ii) human CBS cDNA/pCMV-SPORT6 or (iii) human 3-MST/pCI-HA using TransIT-X2 Dynamic Delivery System (cat. MIR 6004, Mirus Bio, Madison, USA). Two days after

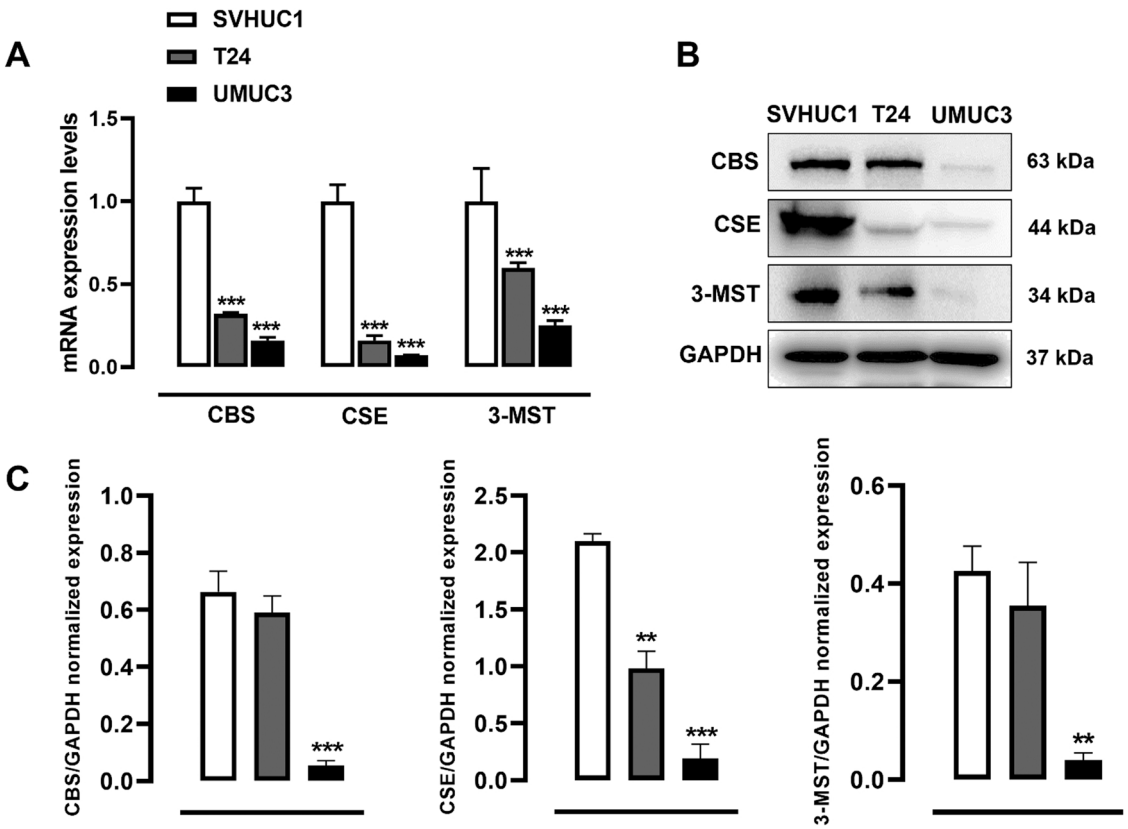

Fig. 1. mRNA and protein expression of CBS, CSE and 3-MST in UC cells. (A) mRNA expression levels of CBS, CSE, and 3-MST in SVHUC1, T24 and UMUC3 cells were evaluated by qPCR analysis. The housekeeping gene (ribosomal protein S16) was used as an internal control to normalize the ct values; (B-C) Representative blots and quantitative analysis of CBS, CSE and 3-MST in SVHUC1, T24 and UMUC3 whole-cell lysates; $^{**}P < 0.01$, $^{***}P < 0.001$ versus SVHUC1.

transfection, cell proliferation and apoptosis were evaluated (see next sections). The overexpression of the genes of interest was evaluated and quantified using qPCR analysis (see supplementary fig. 1).

2.5. Proliferation assay

Cell proliferation was measured by MTT (3-(4,5-dimethylthiazol-2-yl)− 2,5-diphenyltetrazolium bromide) assay. SVHUC1, T24 and UMUC3 cells were seeded on 96-well plates (3×10^3 cells/well). After 24 h, cells were treated with two H_2S-donors (i) DATS (10–30–100 μM) and (ii) GYY4137 (30–100–300 μM) for 72 h before adding MTT (cat. M5655, Merk, Italy) (final concentration 5 mg/ml in PBS). Cells were incubated for an additional 3 h at 37 °C. After this time, cells were lysed and formazan salts resulting from MTT reduction were solubilized with a solution containing 50% (vol/vol) N,N-dimethyl formamide, 20% (wt/vol) sodium dodecylsulfate with an adjusted pH of 4.5. The absorbance was measured using a microplate spectrophotometer (Thermo Scientific Multiskan GO, Thermo Fisher Scientific, MA, USA) equipped with a 570-nm filter. None of the compounds tested under the same experimental conditions had a cytotoxic effect on SVHUC1.

2.6. Flow cytometry

Apoptosis was measured using the BD Pharmingen™ FITC Annexin V Apoptosis Detection Kit I (cat. 556547, BD Biosciences, Franklin Lakes, NJ, USA) according to the manufacturer's instructions. UMUC3 cells were seeded (2.5×10^5 cell/well) in 35 mm culture dishes. On the day next, the cells were treated with DATS (100 μM) for 24 and 48 h. After this time, UMUC3 cells were collected and washed twice with PBS and stained with Annexin V-FITC/Propidium Iodide (PI). Flow cytometry analysis was performed using a BriCyte flow cytometer (Mindray, Italy) as described previously [29]. A minimum of 50000 events for each sample were collected and data were analyzed using FlowJo v10 software (Tree Star, Ashland, OR, USA).

2.7. Cell cycle analysis

Cell cycle analysis was measured using BD Pharmingen™ FITC BrdU Flow Kit (cat. 559619, BD Biosciences, Franklin Lakes, NJ, USA). For these experiments, UMUC3 cells were seeded in a 6-well plate (1.5×10^5 cells/well) and treated after 24 h with DATS (100 μM) for 24 and 48 h. Cells were analyzed using BriCyte flow cytometer (Mindray, Trezzano sul Naviglio Italy), gated based on forward and side scatter to separate debris, and then the cellular events were further gated based on their BrdU and 7-AAD content. Quantification of results was made using FlowJo v10 software (Tree Star, Ashland, OR, USA) and expressed as fold change of the cells in each cell cycle phase.

2.8. Wound healing assay

UMUC3 cells were seeded in 6-well plates (3×10^5 cells/ well). Once the cells reached 90% confluence, DATS (1–3–10 μM) was added and a wound area was generated by scraping the cell monolayer with a sterile 200 μl pipette tip. Subsequently, the cells were incubated at 37 °C in 5% CO_2. The width of the wounded area was monitored and photographed with an inverted microscope (20-fold magnification) at the time zero point and after 24 h, 48 h, and 72 h of treatment. The wounded area was measured using Image J software (version 1.52a, U.S. National Institutes of Health) [30].

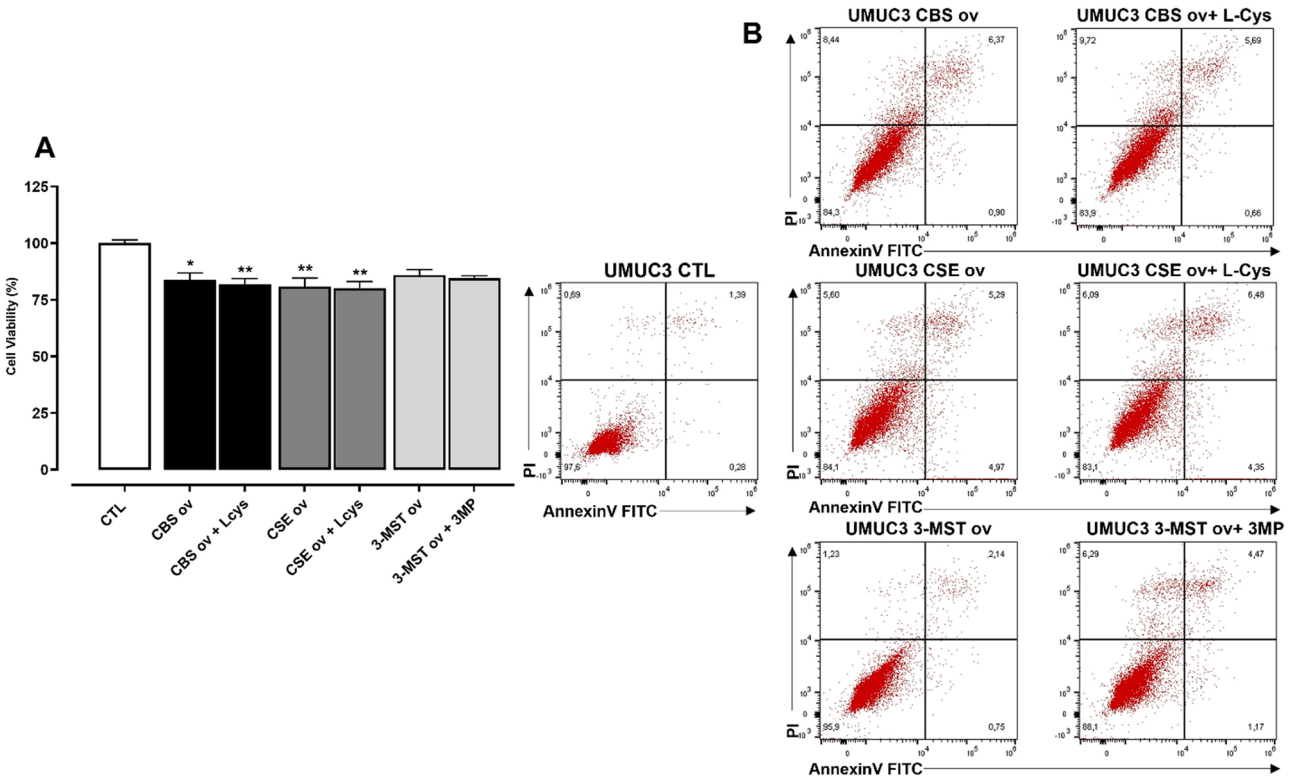

Fig. 2. Overexpression (ov) of CBS, CSE and 3-MST genes in UMUC3 cells. (A) MTT proliferation assay performed in CBS, CSE and 3-MST transfected UMUC3 cells exposed or not to L-Cysteine and 3-MP. Each column is the mean±SEM of three independent experiments, each performed in quadruplicate. *P < 0.05, **P < 0.01 versus CTL; (B) Flow cytometric analysis of apoptosis detected by Annexin V/propidium iodide (PI) staining in UMUC3 cells performed in the same cell conditions.

2.9. Clonogenic assay

UMUC3 cells were seeded in 6-well plates (1×10^3 cells/well) on the day next treated with DATS (1–3–10 μM) and allowed to form colonies for 14 days. Once the colonies were formed, after washing with PBS, the cells were fixed with 4% paraformaldehyde and stained with 0.5% crystal violet. Colonies composed of more than 50 cells were manually counted under the microscope and captured by a digital camera.

2.10. Statistical analysis

Data are expressed as mean ± SEM of n experiments. Data were analyzed and presented using GraphPad Prism 5.0 software (San Diego, CA, USA). Significance was determined using Student's 2-tailed t-test. Results were considered significant at P values less than 0.05 and are labeled with a single asterisk. In addition, P values less than 0.01 and 0.001 are indicated with double and triple asterisks, respectively.

3. Results

3.1. CBS, CSE, and 3-MST genes and proteins expression are reduced in human urothelial carcinoma cell lines

To understand the potential role of the H_2S pathway in urothelial carcinoma we first analyzed the expression levels of CBS, CSE, and 3-MST genes in normal human uroepithelial cells (SVHUC1) as well as in two distinct human urothelial carcinoma cell lines (T24 and UMUC3) by using real-time PCR (qPCR) and western blot analysis. As shown in Fig. 1A, the mRNA expression level of all three genes was robustly lower in T24 and UMUC3 cells, as compared to control SVHUC1 cells. This result was also confirmed by western blot analysis (Fig. 1B-C).

3.2. Overexpression of CBS and CSE inhibits urothelial carcinoma cell proliferation

To assess whether CBS, CSE, and 3-MST play a role in urothelial carcinoma cell proliferation, we performed the first experiments in UMUC3 cells that were selected for their extremely low expression of CBS, CSE, and 3-MST. In particular, in these cells, CBS, CSE, and 3-MST were transiently and separately overexpressed to understand their role in cell proliferation. As shown in Fig. 2A, we found that in both CBS- and CSE-transfected UMUC3 cells, the proliferation was significantly lower (about 20%) as compared with control cells. While in 3-MST transfected UMUC3 cells we did not observe significant changes (Fig. 2A). Moreover, in presence of L-cysteine (1 mM), which is a substrate for these enzymes, the anti-proliferative effect of CBS, CSE in transfected UMUC3 cells was not further changed. In addition, there were no changes in presence of 3-MP (10 μM), the substrate for 3-MST (Fig. 2A). Next, to clarify whether the inhibition of cell proliferation observed in CBS and CSE overexpressing cells was associated or not with apoptosis, we performed a cytofluorimetric analysis by using Annexin V/PI dual staining. As shown in Fig. 2B, CBS and CSE overexpression, either alone or in presence of L-cysteine, caused a slight, but significant induction of cell apoptosis. While in 3-MST transfected UMUC3 cells the presence or not of 3-MP did not affect cell apoptosis.

3.3. Exogenous H_2S inhibits proliferation, induces apoptosis, and causes cell cycle arrest of human urothelial carcinoma cells

Since substantial differences have been found in the current literature between endogenously generated and exogenously administered hydrogen sulfide, we assessed the effect on cell proliferation of two H_2S-donors, the natural compound DATS and the synthetic GYY4137 (Fig. 3). Both DATS and GYY4137 did not affect SVHUC1 cell proliferation, however it inhibited growth of T24 and UMUC3 cells in

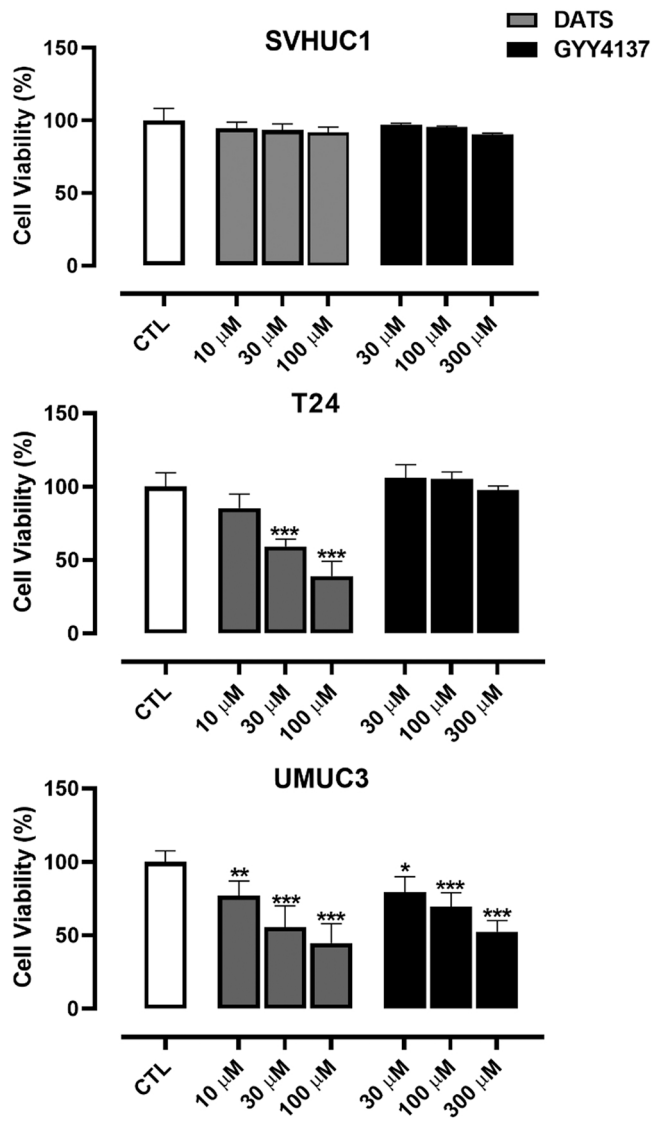

Fig. 3. Effect of two H_2S-donors, DATS and GYY4137, on SVHUC1, T24 and UMUC3 cell proliferation. Cell proliferation was measured using the MTT assay and evaluated at 72 h. Each experiment (n = 3) was run in quadruplicate. *P < 0.05; **P < 0.01; ***P < 0.001 vs. CTL.

concentration-dependent manner with IC50 77 μM and IC50 278 μM, respectively. The antiproliferative effect of DATS in UMUC3 cells was further investigated by FACS analysis using Annexin V/PI double staining. Using this approach, we found that DATS (100 μM) induced UMUC3 cell death by apoptosis in a time-dependent manner (Fig. 4 A). In particular, after 48 h, almost 50% of the cells were in apoptosis. This effect was confirmed by the time-dependent cleavage of Caspase-3, the main effector caspase, and of its substrate poly (adenosine diphosphate-ribose) polymerase (PARP) (Fig. 4B). Additionally, we found that DATS decreased the expression of the two anti-apoptotic proteins X-chromosome-linked inhibitor of apoptosis protein (XIAP) and B-cell lymphoma gene-2 (Bcl-2) (Fig. 4C-D). Furthermore, we found that DATS (100 μM) in UMUC3 cells caused a time-dependent arrest in G0/G1-phase (Fig. 5 A). This latter effect was further confirmed by western blot analysis showing that DATS in UMUC3 cells inhibited the expression of cyclinD1 and Cyclin-Dependent Kinase 4 (CDK4), which are both factors promoting cell proliferation (Fig. 5B-C).

3.4. DATS promotes autophagy in human urothelial carcinoma cells

Recently, several studies have shown that autophagy is a promising target for developing anticancer therapeutic agents [31]. Thus, we explored whether the action of DATS could involve autophagy in human urothelial carcinoma cells. Notably, we found that DATS (100 μM) promoted autophagy in UMUC3 cells in a time-dependent manner, as reflected by the increased expression of autophagy-related genes such as ATG13, BECN1, BNIP3, LAMP1, ULK1, mTOR (Fig. 6 A). Additionally, by western blot analysis, we found that DATS significantly increased the expression of LC3II protein, the lipidated form of the LC3I (Fig. 6B), and concomitantly decreased the expression of p62, which are considered key regulators of autophagosome formation and activity (Fig. 6 C).

3.5. DATS suppresses epithelial-mesenchymal transition

The process of cancer cell transition from an epithelial-adhered phenotype to a mesenchymal phenotype has been shown to potentiate migration, invasion, resistance, and metastasis of cancers [32,33]. Therefore, using quantitative PCR (qPCR), we measured in UMUC3 cells exposed to DATS, the expression of canonical mesenchymal markers including SLUG and ZEB1. Intriguingly, DATS (100 μM) significantly inhibited the mRNA levels of SLUG (by about 50%) and ZEB-1 (by about 30%) (Fig. 7 A). Additionally, we found that DATS, in the same cell conditions, promoted the expression of E-Cadherin, a well-known marker of epithelial cells, and inhibited the mesenchymal markers Caveolin-1 and Vimentin (Fig. 7B-C).

3.6. DATS inhibits cell migration and colony formation of human urothelial carcinoma cells

Migration and invasiveness of tumor cells are closely related to cancer metastasis. The antimetastatic activity of DATS was investigated by evaluating its ability to inhibit some of the malignant features of urothelial carcinoma cells, in vitro. A wound-healing assay was performed to determine whether concentrations of DATS that do not inhibit proliferation or cause apoptosis, interfere with UMUC3 cells motility. Treatment with DATS (1–3–10 μM) significantly and time-dependently reduced UMUC3 cells migration as compared to untreated cells (Fig. 8A-B). Furthermore, DATS significantly reduced the colony formation ability of UMUC3 cells. This data correlates with the capacity of tumor cells to produce progeny and form metastasis in vivo [34]. As shown in Fig. 8 C DATS (1–3–10 μM) significantly reduces the number of colonies as well as focus diameter compared to untreated cells in a concentration-dependent manner.

4. Discussion

H_2S pathway is involved in both cancer suppression [35–38] and progression [39,40]. Despite the recent discoveries, the role of this gasotransmitter in cancer has been not fully elucidated. Urothelial carcinoma (UC) is the most common malignancy of the urinary tract. It has been estimated that only in 2020, there have been ~573,000 new cases with 213,000 deaths worldwide [41]. In the current scientific literature, there are only few papers showing an involvement of H_2S pathway in bladder cancer. The present evidence is that the expression of H_2S producing enzymes negatively correlates with cancer development and progression [42,43].

In this study, we show that in two distinct carcinoma cell lines, namely T24 and UMUC3, the expression of CBS, CSE, and 3-MST is much lower than in control cells i.e. SVHUC1. To understand if the down-regulation of H_2S pathway is involved in contrasting cancer development, we overexpressed all three enzymes. The overexpression of CBS or CSE in UC cells inhibits cell proliferation and promotes apoptosis. Whereas overexpression of 3-MST had no effects on both proliferation and apoptosis revealing that the activity of this enzyme is not involved

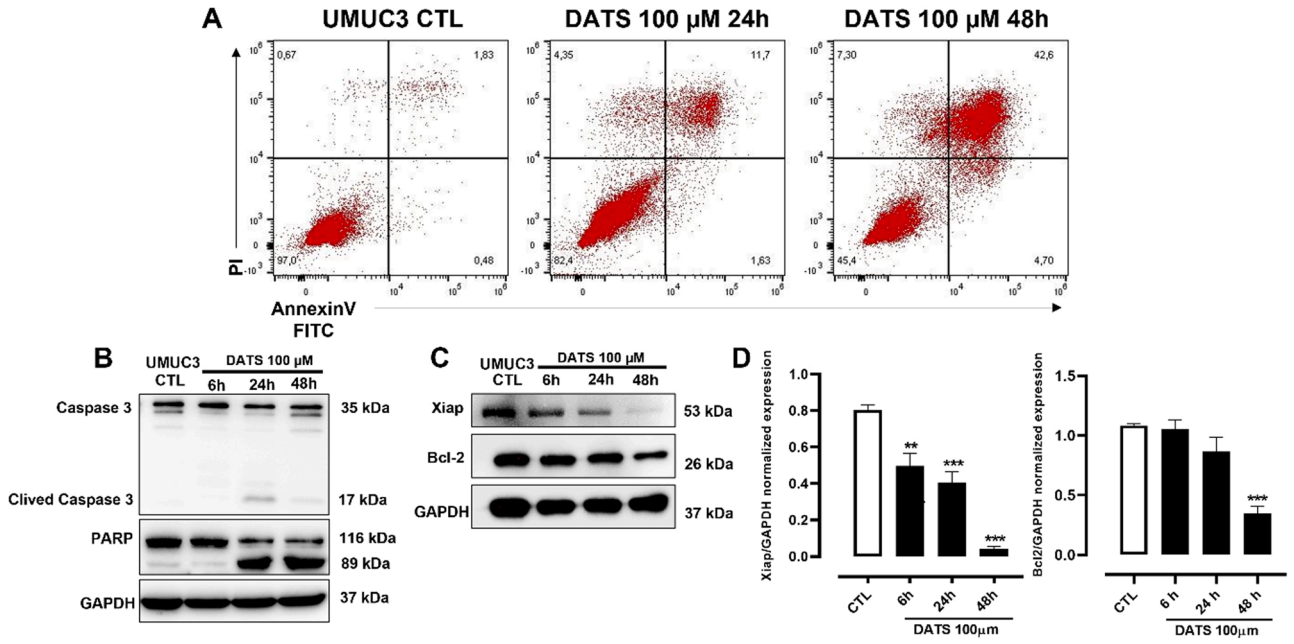

Fig. 4. DATS induces apoptosis in UMUC3 cells. (A) Flow cytometric analysis of apoptosis detected by Annexin V/propidium iodide (PI) staining in UMUC3 cells treated with DATS (100 μM) for 24 and 48 h; (B) western blot analysis of caspase-3, PARP and of (C) XIAP and Bcl-2 carried out on UMUC3 whole-cell lysates following the treatment with DATS (100 μM) for 6, 24 and 48 h; (D) quantitative analysis of XIAP and Bcl-2, GAPDH was detected as loading control. The data shown are representative of three independent experiments (n = 3) with similar results. **P < 0.01; ***P < 0.001 versus CTL.

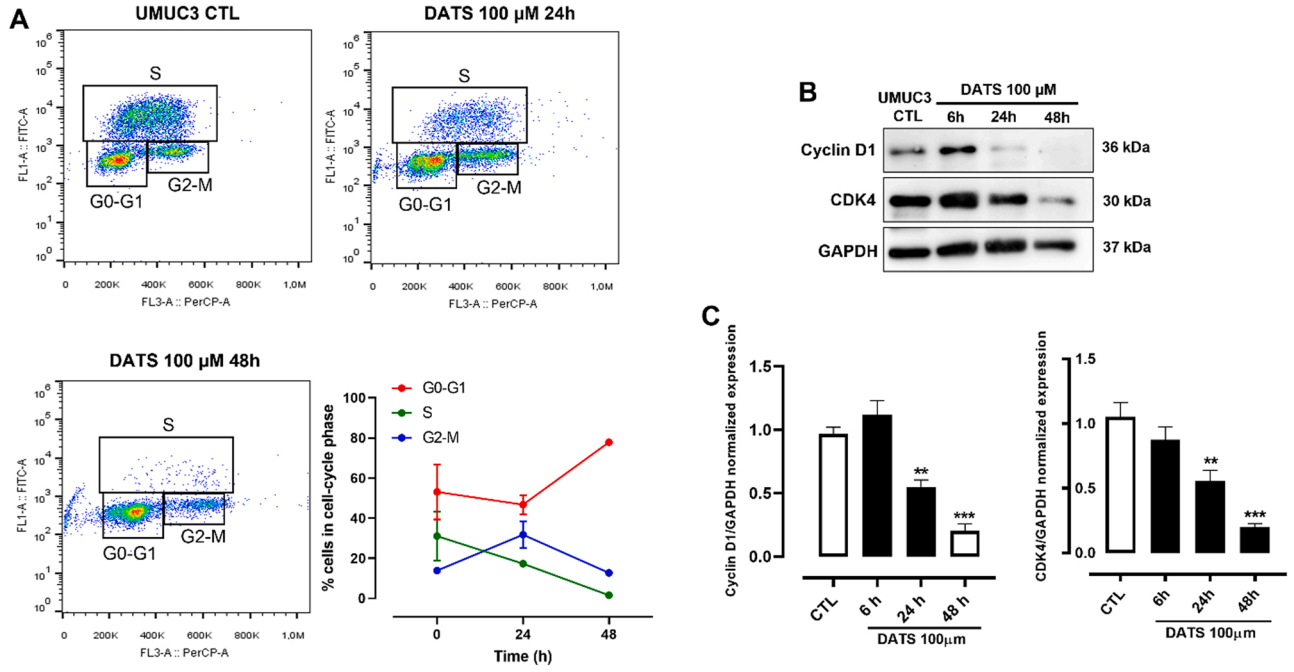

Fig. 5. DATS induces cell cycle arrest in UMUC3 cells. (A) Representative density plots and cell percentage, indicating the G0/G1, S and G2/M phase distribution of UMUC3 cells treated or not with DATS (100 μM) for 24 and 48 h; (B) representative western blot, and (C) relative quantitative analysis of cyclin D1 and CDK4 proteins measured in UMUC3 whole-cell lysates following the treatment with DATS (100 μM) for 6, 24 and 48 h. GAPDH was detected as loading control. Each data point was obtained from at least three independent determinations for each experimental condition. **P < 0.01; ***P < 0.001 versus CTL.

or is not sufficient alone to control these cellular processes. Thus, in UC cells increasing the endogenous production of CBS and CSE-derived hydrogen sulfide have a beneficial effect, suggesting that H_2S donors (exogenous) could act as an efficacious therapeutic replacement.

Exogenous H_2S has two opposite effects on cancer cell growth that is strictly linked to (i) concentration, high vs low, and (ii) the time of exposure. Overall, the treatment with a relatively high concentration of H_2S-donors for a long time (over 24 h) has been reported to inhibit cancer cell growth in different types of tumors suggesting that slow-releasing H_2S donors could be a promising therapeutic strategy in antineoplastic therapy [17,25,44]. Here the two slow H_2S-donors, GYY4137 and DATS, inhibited the growth of T24 and UMUC3 carcinoma cells in a time and concentration-dependent manner. This is in line with the hypothesis that a consistent concentration of H_2S over a certain

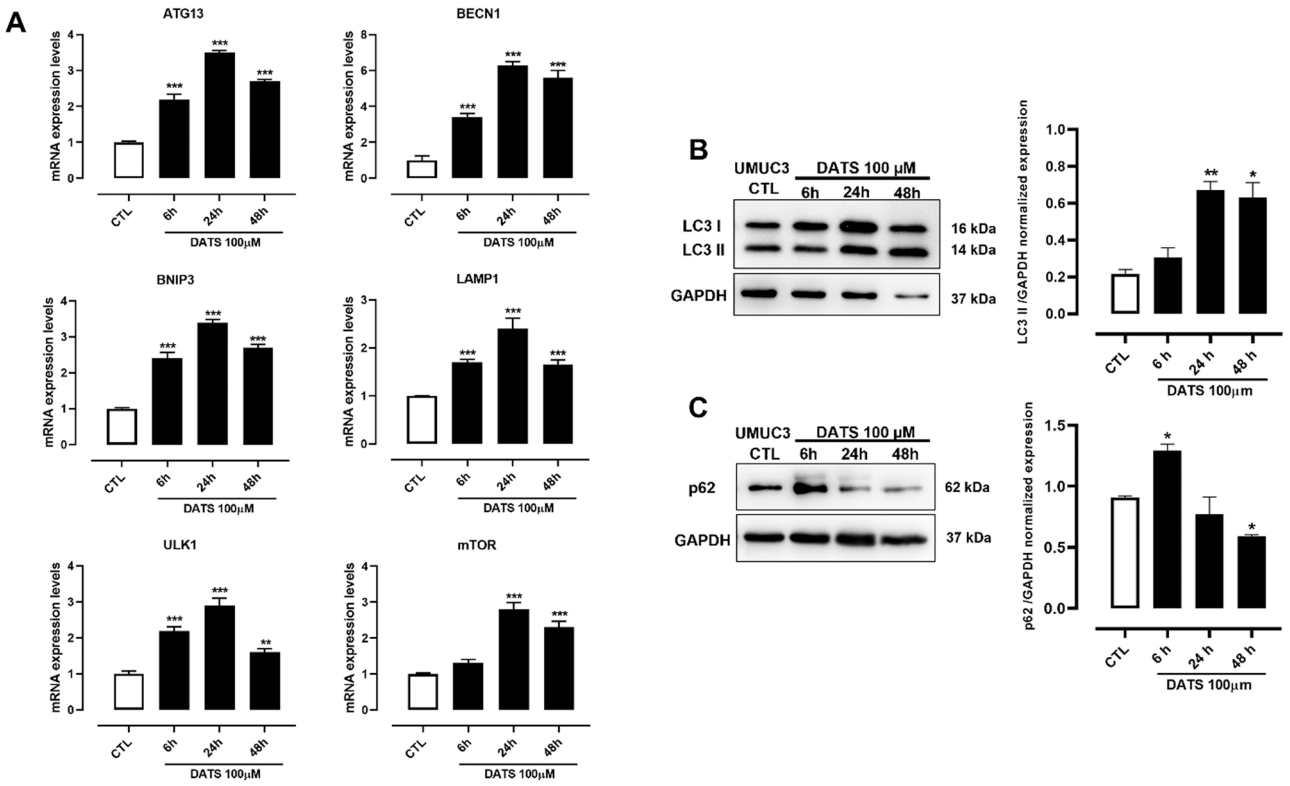

Fig. 6. DATS induces autophagy in UMUC3 cells. (A) mRNA expression levels of ATG13, BECN1, BNIP3, LAMP1, ULK1, mTOR in UMUC3 cells following the treatment with DATS (100 μM) for 6, 24 and 48 h; (B-C) Representative blots and quantitative analysis of LC3 and P62 proteins measured in UMUC3 following the treatment with DATS (100 μM) for 6, 24 and 48 h. GAPDH was detected as a loading control. Each data point was obtained from at least three independent determinations for each experimental condition. *P < 0.05; **P < 0.01 versus CTL.

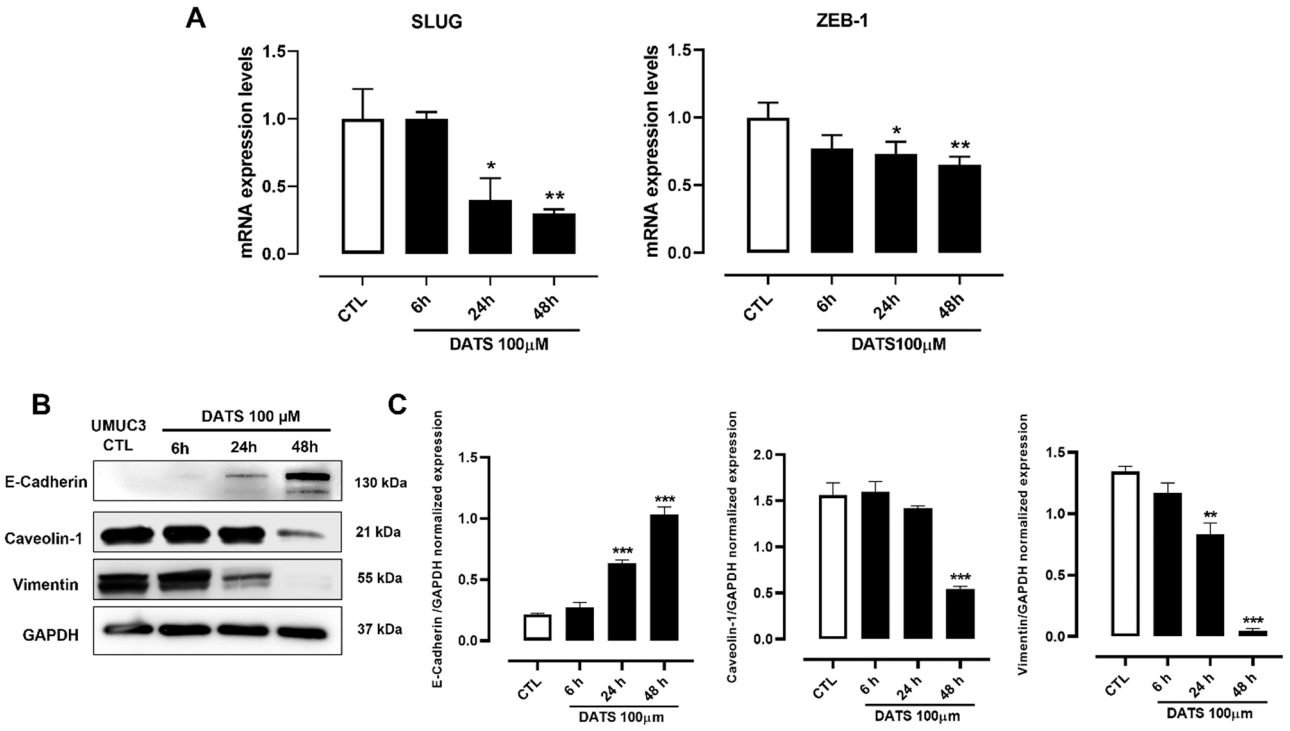

Fig. 7. DATS suppresses epithelial-mesenchymal transition. (A) mRNA expression levels of SLUG and ZEB1 in UMUC3 cells following the treatment with DATS (100 μM) for 6, 24 and 48 h; (B-C) representative western blot, and relative quantitative analysis of E-Cadherin, Caveolin-1 and Vimentin carried out on UMUC3 whole-cell lysates following the treatment with DATS (100 μM) for 6, 24 and 48 h. GAPDH was detected as the loading control. The data shown are representative of three independent experiments (n = 3) with similar results. *P < 0.05; **P < 0.01; ***P < 0.001 versus CTL.

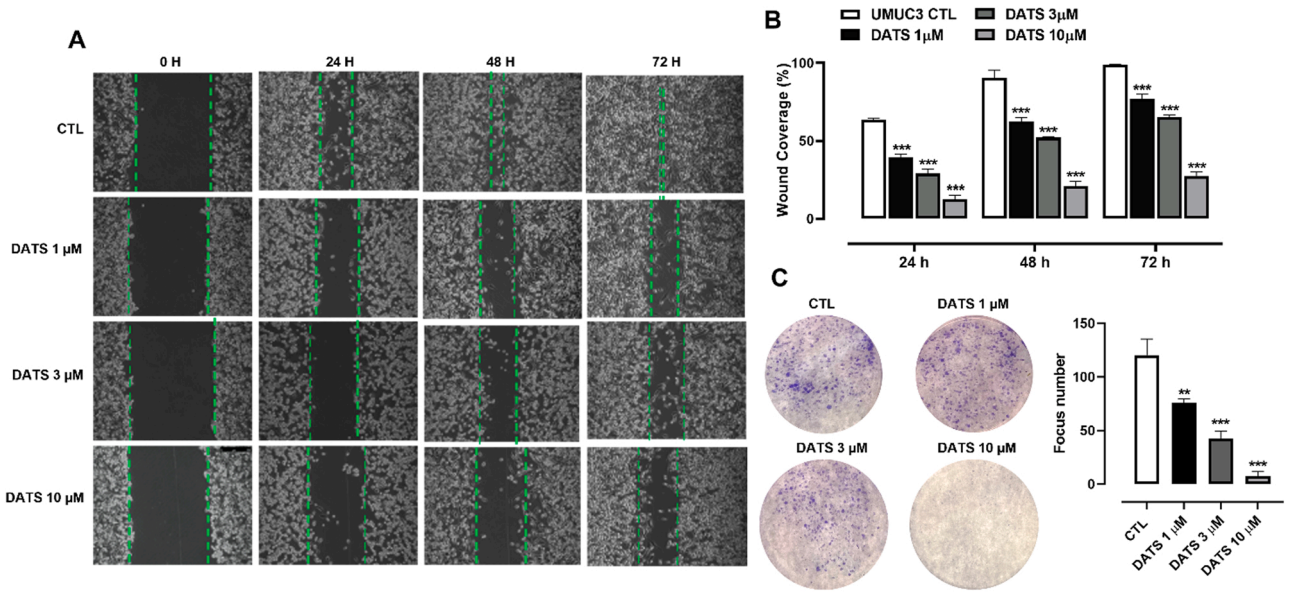

Fig. 8. DATS inhibits the migration and colony formation ability of UMUC3 cells. (A) Representative photographs of migratory UMUC3 cells treated with DATS (1–3–10 μM) at 0, 24, 48, and 72 h later. (B) The scratched areas were quantified in three random fields in each treatment. Data are shown as mean ± SEM of three independent experiments (n = 3). ***P < 0.001 versus CTL. (C) Representative photographs and the average number of UMUC3 stained colonies following the treatment with DATS (1–3–10 μM). Data are shown as mean ± SEM of three independent experiments (n = 3). **P < 0.01, ***P < 0.001 versus CTL.

period of contact time is necessary to replace or mimic the endogenous H_2S effect.

To follow this hypothesis, we used DATS since its H_2S-delivering property has been fully characterized as a thiol-dependent mechanism [45].

As we have shown, DATS through the release of H_2S in UC cells halts the proliferation and concomitantly induces apoptosis. This is clearly evident as revealed by the cytofluorimetric assay with Annexin V/PI dual staining and western blot for Caspase-3 and its substrate PARP. Moreover, the antiapoptotic effect of DATS leads also to the inhibition of the two anti-apoptotic proteins XIAP and Bcl-2. Next, to gain further insights into the mechanism of action of DATS we measured its effect on cell cycle progression. DATS arrested UC cell cycle in the G0/G1 phase, with a concomitant decrease in the number of cells in the S phase. This latter effect was coupled with a reduction in the expression of cyclin D1/CDK4 complex normally driving the transition from G1 to S phase. Thus, the behavior of exogenous H_2S on UC recapitulates the pattern already shown in other types of cancer [8].

In recent years, it has been reported that programmed cell death is not confined to apoptosis and that cells use different pathways for active self-destruction. Another important programmed cell death pathway is autophagy [46]. Increasing evidence has indicated that autophagy may be a double edge sword in carcinogenesis and anticancer therapies [47–49]. On one hand, unfolded or aggregated proteins and organelles are degraded by autophagy to maintain intracellular metabolic homeostasis, which may make cancer cells insensitive to chemotherapy drugs [50]. On the other hand, apoptosis may be triggered by autophagy thereby inhibiting cancer progression [51]. Therefore, apoptosis and autophagy may be cooperative to determine cell fate. Here, we first document that DATS induces autophagy in UC cells, as reflected by the increased expression of autophagy-related genes such as ATG13, BECN1, BNIP3, LAMP1, ULK1, mTOR. Moreover, DATS reduced the expression of p62, involved in the lysosome-dependent degradation system, and enhanced the expression of LC3-II, used as a marker of complete activation of the autophagosome.

Epithelial-to-mesenchymal transition (EMT), is a pathological transition that epithelial cells undergo profound morphogenetic changes, promoting tumor invasion and dissemination [52,53]. EMT process is initiated by several transcription factors [54]. Among these, both SLUG, and ZEB1 were inhibited by DATS. Activation of these factors also leads to the suppression of E-cadherin transcription that is increased by DATS. Conversely, the mesenchymal markers Vimentin and Caveolin-1 were inhibited. Thus, exogenous H_2S has a time-dependent effect on epithelial-mesenchymal transition in UC cells. EMT is also involved in metastatic processes [55]. The molecular studies indicating a beneficial effect of H_2S on EMT, are further supported by the finding that DATS reduces migration and clonogenic ability of human UC cells in an in vitro test of cell invasion.

5. Conclusions

H_2S pathway is impaired in UC contributing to cancer development. This is indicated by the finding that by increasing the amount of the endogenous production or by delivering exogenous H_2S is possible to activate the molecular machinery that limits cancer spreading. In particular, the fully characterized H_2S donor DATS, reduced UC cell proliferation inducing autophagy and apoptosis, and concomitantly inhibited cell cycle, cell migration, and EMT. One limitation is that our study did not include data on human primary cells harvested from UC patients. However, it is feasible that molecules releasing H_2S can represent a possible novel additive therapeutic approach to human bladder cancer therapies.

Source of funding

This work was supported by Progetto Campania Oncoterapie, POR Campania FESR 2014–2020.

CRediT authorship contribution statement

Elisabetta Panza: Conceptualization, Data curation, Methodology, Formal analysis, Investigation, Visualization, Supervision, Writing – review & editing. **Ivana Bello**: Data curation, Methodology, Formal analysis, Investigation, Visualization. **Martina Smimmo**: Data curation, Methodology, Formal analysis, Investigation, Visualization. **Vincenzo Brancaleone**: Data curation, Methodology, Formal analysis, Investigation, Visualization. **Emma Mitidieri**: Data curation, Methodology, Formal analysis, Investigation, Visualization. **Mariarosaria Bucci**:

Conceptualization, Data curation, Formal analysis, Investigation. **Giuseppe Cirino**: Conceptualization, Data curation, Visualization, Supervision, Writing – review & editing. **Raffaella Sorrentino**: Conceptualization, Data curation, Formal analysis, Supervision. **Roberta d'Emmanuele di Villa Bianca**: Conceptualization, Data curation, Formal analysis, Supervision.

Author contributions

EP, IB, MS, and VB formulated the current study and executed the experiments. EM, MB, RS and RdEVB help in data curation. EP and GC wrote and reviewed the manuscript. Final form of the manuscript was approved by all the authors.

Conflict of interest statement

The authors declare no conflict of interest.

Data availability

Data will be made available on request.

Appendix A. Supporting information

Supplementary data associated with this article can be found in the online version at doi:10.1016/j.biopha.2022.113137.

References

[1] K. Saginala, A. Barsouk, J.S. Aluru, P. Rawla, S.A. Padala, A. Barsouk, Epidemiology of bladder cancer, Med. Sci. 8 (2020) 15, https://doi.org/10.3390/medsci8010015.

[2] D.S. Kaufman, W.U. Shipley, A.S. Feldman, Bladder cancer, Lancet 374 (2009) 239–249, https://doi.org/10.1016/S0140-6736(09)60491-8.

[3] G. Niegisch, H. Gerullis, S.-W. Lin, J. Pavlova, A. Gondos, A. Rudolph, G. Haas, N. Hennies, M.W. Kramer, A real-world data study to evaluate treatment patterns, clinical characteristics and survival outcomes for first- and second-line treatment in locally advanced and metastatic urothelial cancer patients in Germany, J. Cancer 9 (2018) 1337–1348, https://doi.org/10.7150/jca.23162.

[4] M.D. Galsky, J.Á.A. Arija, A. Bamias, I.D. Davis, M. De Santis, E. Kikuchi, X. Garcia-Del-Muro, U. De Giorgi, M. Mencinger, K. Izumi, S. Panni, M. Gumus, M. Özgüroğlu, A.R. Kalebasty, S.H. Park, B. Alekseev, F.A. Schutz, J.-R. Li, D. Ye, N. J. Vogelzang, S. Bernhard, D. Tayama, S. Mariathasan, A. Mecke, A. Thåström, E. Grande, IMvigor130 Study Group, Atezolizumab with or without chemotherapy in metastatic urothelial cancer (IMvigor130): a multicentre, randomised, placebo-controlled phase 3 trial, Lancet 395 (2020) 1547–1557, https://doi.org/10.1016/S0140-6736(20)30230-0.

[5] T. Powles, S.H. Park, E. Voog, C. Caserta, B.P. Valderrama, H. Gurney, H. Kalofonos, S. Radulović, W. Demey, A. Ullén, Y. Loriot, S.S. Sridhar, N. Tsuchiya, E. Kopyltsov, C.N. Sternberg, J. Bellmunt, J.B. Aragon-Ching, D. P. Petrylak, R. Laliberte, J. Wang, B. Huang, C. Davis, C. Fowst, N. Costa, J. A. Blake-Haskins, A. di Pietro, P. Grivas, Avelumab maintenance therapy for advanced or metastatic urothelial carcinoma, N. Engl. J. Med. 383 (2020) 1218–1230, https://doi.org/10.1056/NEJMoa2002788.

[6] D. Wu, W. Si, M. Wang, S. Lv, A. Ji, Y. Li, Hydrogen sulfide in cancer: Friend or foe? Nitric Oxide 50 (2015) 38–45, https://doi.org/10.1016/j.niox.2015.08.004.

[7] K. Kashfi, The dichotomous role of H2S in cancer cell biology? Déjà vu all over again, Biochem. Pharmacol. 149 (2018) 205–223, https://doi.org/10.1016/j.bcp.2018.01.042.

[8] E.E. Ngowi, A. Afzal, M. Sarfraz, S. Khattak, S.U. Zaman, N.H. Khan, T. Li, Q.-Y. Jiang, X. Zhang, S.-F. Duan, X.-Y. Ji, D.-D. Wu, Role of hydrogen sulfide donors in cancer development and progression, Int. J. Biol. Sci. 17 (2021) 73–88, https://doi.org/10.7150/ijbs.47850.

[9] M.R. Hellmich, C. Szabo, Hydrogen sulfide and cancer, Handb. Exp. Pharmacol. 230 (2015) 233–241, https://doi.org/10.1007/978-3-319-18144-8_12.

[10] C. Szabo, C. Coletta, C. Chao, K. Módis, B. Szczesny, A. Papapetropoulos, M. R. Hellmich, Tumor-derived hydrogen sulfide, produced by cystathionine-β-synthase, stimulates bioenergetics, cell proliferation, and angiogenesis in colon cancer, Proc. Natl. Acad. Sci. USA 110 (2013) 12474–12479, https://doi.org/10.1073/pnas.1306241110.

[11] S. Sen, B. Kawahara, D. Gupta, R. Tsai, M. Khachatryan, S. Roy-Chowdhuri, S. Bose, A. Yoon, K. Faull, R. Farias-Eisner, G. Chaudhuri, Role of cystathionine β-synthase in human breast Cancer, Free Radic. Biol. Med. 86 (2015) 228–238, https://doi.org/10.1016/j.freeradbiomed.2015.05.024.

[12] S. Bhattacharyya, S. Saha, K. Giri, I.R. Lanza, K.S. Nair, N.B. Jennings, C. Rodriguez-Aguayo, G. Lopez-Berestein, E. Basal, A.L. Weaver, D.W. Visscher, W. Cliby, A.K. Sood, R. Bhattacharya, P. Mukherjee, Cystathionine beta-synthase (CBS) contributes to advanced ovarian cancer progression and drug resistance, PLoS One 8 (2013), e79167, https://doi.org/10.1371/journal.pone.0079167.

[13] J. Breza, A. Soltysova, S. Hudecova, A. Penesova, I. Szadvari, P. Babula, B. Chovancova, L. Lencesova, O. Pos, J. Breza, K. Ondrias, O. Krizanova, Endogenous H2S producing enzymes are involved in apoptosis induction in clear cell renal cell carcinoma, BMC Cancer 18 (2018) 591, https://doi.org/10.1186/s12885-018-4508-1.

[14] Y. Xu, N. Ma, P. Wei, Z. Zeng, J. Meng, Expression of hydrogen sulfide synthases and Hh signaling pathway components correlate with the clinicopathological characteristics of papillary thyroid cancer patients, Int. J. Clin. Exp. Pathol. 11 (2018) 1818–1824.

[15] P.K. Chakraborty, B. Murphy, S.B. Mustafi, A. Dey, X. Xiong, G. Rao, S. Naz, M. Zhang, D. Yang, D.N. Dhanasekaran, R. Bhattacharya, P. Mukherjee, Cystathionine β-synthase regulates mitochondrial morphogenesis in ovarian cancer, FASEB J. 32 (2018) 4145–4157, https://doi.org/10.1096/fj.201701095R.

[16] L. Wang, H. Shi, Y. Liu, W. Zhang, X. Duan, M. Li, X. Shi, T. Wang, Cystathionine-γ-lyase promotes the metastasis of breast cancer via the VEGF signaling pathway, Int. J. Oncol. 55 (2019) 473–487, https://doi.org/10.3892/ijo.2019.4823.

[17] E. Panza, P. De Cicco, C. Armogida, G. Scognamiglio, V. Gigantino, G. Botti, D. Germano, M. Napolitano, A. Papapetropoulos, M. Bucci, G. Cirino, A. Ianaro, Role of the cystathionine γ lyase/hydrogen sulfide pathway in human melanoma progression, Pigment Cell Melanoma Res. 28 (2015) 61–72, https://doi.org/10.1111/pcmr.12312.

[18] R. Yang, C. Qu, Y. Zhou, J.E. Konkel, S. Shi, Y. Liu, C. Chen, S. Liu, D. Liu, Y. Chen, E. Zandi, W. Chen, Y. Zhou, S. Shi, Hydrogen sulfide promotes Tet1- and Tet2-mediated Foxp3 demethylation to drive regulatory T cell differentiation and maintain immune homeostasis, Immunity 43 (2015) 251–263, https://doi.org/10.1016/j.immuni.2015.07.017.

[19] L.-Y. Chen, R.-L. Huang, M.W. Chan, P.S. Yan, T.-S. Huang, R.-C. Wu, Y. Suryo Rahmanto, P.-H. Su, Y.-C. Weng, J.-L. Chou, T.-K. Chao, Y.-C. Wang, I.-M. Shih, H.-C. Lai, TET1 reprograms the epithelial ovarian cancer epigenome and reveals casein kinase 2α as a therapeutic target, J. Pathol. 248 (2019) 363–376, https://doi.org/10.1002/path.5266.

[20] C. Feng, Y. Luo, Y. Nian, D. Liu, X. Yin, J. Wu, J. Di, R. Zhang, J. Zhang, Diallyl disulfide suppresses the inflammation and apoptosis resistance induced by DCA through ROS and the NF-κB signaling pathway in human barrett's epithelial cells, Inflammation 40 (2017) 818–831. ⟨https://doi.org/10.1007/s10753-017-0526-4⟩.

[21] S. Lu, Y. Gao, X. Huang, X. Wang, GYY4137, a hydrogen sulfide (H_2S) donor, shows potent anti-hepatocellular carcinoma activity through blocking the STAT3 pathway, Int. J. Oncol. 44 (2014) 1259–1267, https://doi.org/10.3892/ijo.2014.2305.

[22] C.-Y. Ho, Y.-T. Cheng, C.-F. Chau, G.-C. Yen, Effect of diallyl sulfide on in vitro and in vivo Nrf2-mediated pulmonic antioxidant enzyme expression via activation ERK/p38 signaling pathway, J. Agric. Food Chem. 60 (2012) 100–107, https://doi.org/10.1021/jf203800d.

[23] L. Lohninger, L. Tomasova, M. Praschberger, M. Hintersteininger, T. Erker, B.M. K. Gmeiner, H. Laggner, Hydrogen sulphide induces HIF-1α and Nrf2 in THP-1 macrophages, Biochimie 112 (2015) 187–195, https://doi.org/10.1016/j.biochi.2015.03.009.

[24] H. Wang, N. Sun, X. Li, K. Li, J. Tian, J. Li, Diallyl trisulfide induces osteosarcoma cell apoptosis through reactive oxygen species-mediated downregulation of the PI3K/Akt pathway, Oncol. Rep. 35 (2016) 3648–3658, https://doi.org/10.3892/or.2016.4722.

[25] P. De Cicco, E. Panza, C. Armogida, G. Ercolano, O. Taglialatela-Scafati, Y. Shokoohinia, R. Camerlingo, G. Pirozzi, V. Calderone, G. Cirino, A. Ianaro, The hydrogen sulfide releasing molecule acetyl deacylasadisulfide inhibits metastatic melanoma, Front. Pharmacol. 8 (2017) 65, https://doi.org/10.3389/fphar.2017.00065.

[26] Z. Yue, X. Guan, R. Chao, C. Huang, D. Li, P. Yang, S. Liu, T. Hasegawa, J. Guo, M. Li, Diallyl disulfide induces apoptosis and autophagy in human osteosarcoma MG-63 cells through the PI3K/Akt/mTOR pathway, Molecules 24 (2019), E2665, https://doi.org/10.3390/molecules24142665.

[27] J.-H. Kang, Y.-S. Jang, H.J. Lee, C.-Y. Lee, D.Y. Shin, S.H. Oh, Inhibition of STAT3 signaling induces apoptosis and suppresses growth of lung cancer: good and bad, Lab Anim. Res. 35 (2019) 30, https://doi.org/10.1186/s42826-019-0030-0.

[28] Omer Faruk Hatipoglu, Kursat Oguz Yaykasli, Mustafa Dogan, Mustafa Dogan, Mehmet Gunduz, NF-κB and MAPKs are involved in resistin-caused ADAMTS-5 induction in human chondrocytes, Clin. Investig. Med. 38 (4) (2015) 248–254.

[29] M.Y. Putra, A. Ianaro, E. Panza, G. Bavestrello, C. Cerrano, E. Fattorusso, O. Taglialatela-Scafati, Sinularioside, a triacetylated glycolipid from the Indonesian soft coral Sinularia sp., is an inhibitor of NO release, Bioorg. Med. Chem. Lett. 22 (2012) 2723–2725, https://doi.org/10.1016/j.bmcl.2012.02.102.

[30] O. Bender, E.J. Llorent-Martínez, G. Zengin, A. Mollica, R. Ceylan, L. Molina-García, M.L. Fernández-de Córdova, A. Atalay, Integration of in vitro and in silico perspectives to explain chemical characterization, biological potential and anticancer effects of Hypericum salsugineum: a pharmacologically active source for functional drug formulations, PLoS One 13 (2018), e0197815, https://doi.org/10.1371/journal.pone.0197815.

[31] X. Sui, R. Chen, Z. Wang, Z. Huang, N. Kong, M. Zhang, W. Han, F. Lou, J. Yang, Q. Zhang, X. Wang, C. He, H. Pan, Autophagy and chemotherapy resistance: a promising therapeutic target for cancer treatment, Cell Death Dis. 4 (2013), e838, https://doi.org/10.1038/cddis.2013.350.

[32] S. Lamouille, J. Xu, R. Derynck, Molecular mechanisms of epithelial-mesenchymal transition, Nat. Rev. Mol. Cell Biol. 15 (2014) 178–196, https://doi.org/10.1038/nrm3758.

[33] M. Iwatsuki, K. Mimori, T. Yokobori, H. Ishi, T. Beppu, S. Nakamori, H. Baba, M. Mori, Epithelial-mesenchymal transition in cancer development and its clinical significance, Cancer Sci. 101 (2010) 293–299, https://doi.org/10.1111/j.1349-7006.2009.01419.x.
[34] N.A.P. Franken, H.M. Rodermond, J. Stap, J. Haveman, C. van Bree, Clonogenic assay of cells in vitro, Nat. Protoc. 1 (2006) 2315–2319, https://doi.org/10.1038/nprot.2006.339.
[35] Q. Dong, B. Yang, J.-G. Han, M.-M. Zhang, W. Liu, X. Zhang, H.-L. Yu, Z.-G. Liu, S.-H. Zhang, T. Li, D.-D. Wu, X.-Y. Ji, S.-F. Duan, A novel hydrogen sulfide-releasing donor, HA-ADT, suppresses the growth of human breast cancer cells through inhibiting the PI3K/AKT/mTOR and Ras/Raf/MEK/ERK signaling pathways, Cancer Lett. 455 (2019) 60–72, https://doi.org/10.1016/j.canlet.2019.04.031.
[36] Z.W. Lee, J. Zhou, C.-S. Chen, Y. Zhao, C.-H. Tan, L. Li, P.K. Moore, L.-W. Deng, The slow-releasing hydrogen sulfide donor, GYY4137, exhibits novel anti-cancer effects in vitro and in vivo, PLoS One 6 (2011), e21077, https://doi.org/10.1371/journal.pone.0021077.
[37] S. Sakuma, S. Minamino, M. Takase, Y. Ishiyama, H. Hosokura, T. Kohda, Y. Ikeda, Y. Fujimoto, Hydrogen sulfide donor GYY4137 suppresses proliferation of human colorectal cancer Caco-2 cells by inducing both cell cycle arrest and cell death, Heliyon 5 (2019), e02244, https://doi.org/10.1016/j.heliyon.2019.e02244.
[38] G. Oláh, K. Módis, G. Törö, M.R. Hellmich, B. Szczesny, C. Szabo, Role of endogenous and exogenous nitric oxide, carbon monoxide and hydrogen sulfide in HCT116 colon cancer cell proliferation, Biochem. Pharmacol. 149 (2018) 186–204, https://doi.org/10.1016/j.bcp.2017.10.011.
[39] Y. Zhen, Q. Wu, Y. Ding, W. Zhang, Y. Zhai, X. Lin, Y. Weng, R. Guo, Y. Zhang, J. Feng, Y. Lei, J. Chen, Exogenous hydrogen sulfide promotes hepatocellular carcinoma cell growth by activating the STAT3-COX-2 signaling pathway, Oncol. Lett. 15 (2018) 6562–6570, https://doi.org/10.3892/ol.2018.8154.
[40] Y. Lei, Y. Zhen, W. Zhang, X. Sun, X. Lin, J. Feng, H. Luo, Z. Chen, C. Su, B. Zeng, J. Chen, Exogenous hydrogen sulfide exerts proliferation, anti-apoptosis, angiopoiesis and migration effects via activating HSP90 pathway in EC109 cells, Oncol. Rep. 35 (2016) 3714–3720, https://doi.org/10.3892/or.2016.4734.
[41] H. Sung, J. Ferlay, R.L. Siegel, M. Laversanne, I. Soerjomataram, A. Jemal, F. Bray, Global Cancer Statistics 2020: GLOBOCAN estimates of incidence and mortality worldwide for 36 cancers in 185 countries, CA Cancer J. Clin. 71 (2021) 209–249, https://doi.org/10.3322/caac.21660.
[42] J.-W. Gai, W. Qin, M. Liu, H.-F. Wang, M. Zhang, M. Li, W.-H. Zhou, Q.-T. Ma, G.-M. Liu, W.-H. Song, J. Jin, H.-S. Ma, Expression profile of hydrogen sulfide and its synthases correlates with tumor stage and grade in urothelial cell carcinoma of bladder, Urol. Oncol. 34 (2016), https://doi.org/10.1016/j.urolonc.2015.06.020.
[43] W. Wahafu, J. Gai, L. Song, H. Ping, M. Wang, F. Yang, Y. Niu, N. Xing, Increased H2S and its synthases in urothelial cell carcinoma of the bladder, and enhanced cisplatin-induced apoptosis following H2S inhibition in EJ cells, Oncol. Lett. 15 (2018) 8484–8490, https://doi.org/10.3892/ol.2018.8373.
[44] P. De Cicco, E. Panza, G. Ercolano, C. Armogida, G. Sessa, G. Pirozzi, G. Cirino, J. L. Wallace, A. Ianaro, ATB-346, a novel hydrogen sulfide-releasing anti-inflammatory drug, induces apoptosis of human melanoma cells and inhibits melanoma development in vivo, Pharmacol. Res. 114 (2016) 67–73, https://doi.org/10.1016/j.phrs.2016.10.019.
[45] G.A. Benavides, G.L. Squadrito, R.W. Mills, H.D. Patel, T.S. Isbell, R.P. Patel, V. M. Darley-Usmar, J.E. Doeller, D.W. Kraus, Hydrogen sulfide mediates the vasoactivity of garlic, Proc. Natl. Acad. Sci. USA 104 (2007) 17977–17982, https://doi.org/10.1073/pnas.0705710104.
[46] W. Bursch, A. Ellinger, C. Gerner, U. Fröhwein, R. Schulte-Hermann, Programmed cell death (PCD). Apoptosis, autophagic PCD, or others? Ann. N. Y. Acad. Sci. 926 (2000) 1–12, https://doi.org/10.1111/j.1749-6632.2000.tb05594.x.
[47] S.-Y. Kim, Cancer metabolism: strategic diversion from targeting cancer drivers to targeting cancer suppliers, Biomol. Ther. 23 (2015) 99–109, https://doi.org/10.4062/biomolther.2015.013.
[48] Y. Quan, H. Lei, W. Wahafu, Y. Liu, H. Ping, X. Zhang, Inhibition of autophagy enhances the anticancer effect of enzalutamide on bladder cancer, Biomed. Pharmacother. 120 (2019), 109490, https://doi.org/10.1016/j.biopha.2019.109490.
[49] J. Zhu, Z. Tian, Y. Li, X. Hua, D. Zhang, J. Li, H. Jin, J. Xu, W. Chen, B. Niu, X.-R. Wu, S. Comincini, H. Huang, C. Huang, ATG7 promotes bladder cancer invasion via autophagy-mediated increased ARHGDIB mRNA stability, Adv. Sci. 6 (2019) 1801927, https://doi.org/10.1002/advs.201801927.
[50] S. Chen, S.K. Rehman, W. Zhang, A. Wen, L. Yao, J. Zhang, Autophagy is a therapeutic target in anticancer drug resistance, Biochim. Biophys. Acta 2010 (1806) 220–229, https://doi.org/10.1016/j.bbcan.2010.07.003.
[51] B. Rah, R. Ur Rasool, D. Nayak, S.K. Yousuf, D. Mukherjee, L.D. Kumar, A. Goswami, , PAWR-mediated suppression of BCL2 promotes switching of 3-azido withaferin A (3-AWA)-induced autophagy to apoptosis in prostate cancer cells, Autophagy 11 (2015) 314–331. ⟨https://doi.org/10.1080/15548627.2015.1017182⟩.
[52] L.J. Talbot, S.D. Bhattacharya, P.C. Kuo, Epithelial-mesenchymal transition, the tumor microenvironment, and metastatic behavior of epithelial malignancies, Int. J. Biochem. Mol. Biol. 3 (2012) 117–136.
[53] J. Yang, R.A. Weinberg, Epithelial-mesenchymal transition: at the crossroads of development and tumor metastasis, Dev. Cell 14 (2008) 818–829, https://doi.org/10.1016/j.devcel.2008.05.009.
[54] A. Yadav, B. Kumar, J. Datta, T.N. Teknos, P. Kumar, IL-6 promotes head and neck tumor metastasis by inducing epithelial-mesenchymal transition via the JAK-STAT3-SNAIL signaling pathway, Mol. Cancer Res. 9 (2011) 1658–1667, https://doi.org/10.1158/1541-7786.MCR-11-0271.
[55] K.T. Yeung, J. Yang, Epithelial-mesenchymal transition in tumor metastasis, Mol. Oncol. 11 (2017) 28–39, https://doi.org/10.1002/1878-0261.12017.